

ON THE INTERACTION OF ADENINE WITH IONIZING RADIATION: MECHANISTICAL STUDIES AND ASTROBIOLOGICAL IMPLICATIONS

NICHOLAS L. EVANS¹, CHRIS J. BENNETT^{2,3}, SUSANNE ULLRICH¹, AND RALF I. KAISER^{2,3}

¹ Department of Physics and Astronomy, University of Georgia, Athens, GA 30602, USA

² Department of Chemistry, University of Hawaii at Manoa, Honolulu, HI 96822, USA; ralfk@hawaii.edu

³ UH NASA Astrobiology Institute, University of Hawaii at Manoa, Honolulu, HI 96822, USA

Received 2010 October 7; accepted 2010 December 30; published 2011 March 7

ABSTRACT

The molecular inventory available on the prebiotic Earth was likely derived from both terrestrial and extraterrestrial sources. A complete description of which extraterrestrial molecules may have seeded early Earth is therefore necessary to fully understand the prebiotic evolution which led to life. Galactic cosmic rays (GCRs) are expected to cause both the formation and destruction of important biomolecules—including nucleic acid bases such as adenine—in the interstellar medium within the ices condensed on interstellar grains. The interstellar ultraviolet (UV) component is expected to photochemically degrade gas-phase adenine on a short timescale of only several years. However, the destruction rate is expected to be significantly reduced when adenine is shielded in dense molecular clouds or even within the ices of interstellar grains. Here, biomolecule destruction by the energetic charged particle component of the GCR becomes important as it is not fully attenuated. Presented here are results on the destruction rate of the nucleobase adenine in the solid state at 10 K by energetic electrons, as generated in the track of cosmic ray particles as they penetrate ices. When both UV and energetic charged particle destructive processes are taken into account, the half-life of adenine within dense interstellar clouds is found to be ~ 6 Myr, which is on the order of a star-forming molecular cloud. We also discuss chemical reaction pathways within the ices to explain the production of observed species, including the formation of nitriles ($R-C\equiv N$), epoxides ($C-O-C$), and carbonyl functions ($R-C=O$).

Key words: astrobiology – astrochemistry – methods: laboratory – molecular processes – radiation mechanisms: non-thermal

Online-only material: color figures

1. INTRODUCTION

Deoxyribonucleic acid (DNA) and ribonucleic acid (RNA)—today responsible for storing and passing on our genetic information—are complex organic polymers composed of nitrogen-rich heterocyclic (N-heterocyclic) nucleobases attached to a sugar-phosphate backbone. Discussion still continues as to whether life first evolved in an “RNA world” as proposed by Gilbert (1986) or whether self-replicating proteins evolved first, and later learned to use DNA/RNA to safeguard sensitive genetic information (Ikehara 1999; Lacey et al. 1999; Rode 1999). The subsequent transition from either starting scenario to the DNA/RNA/protein world of extant life is yet to be fully understood (Poole et al. 1998; Freeland et al. 1999; Dworkin et al. 2003; Orgel 2004). However, it is certain that organisms began accumulating and replicating DNA/RNA at some point along the evolutionary timeline (Darnell & Doolittle 1986; Griffith 2009). Hence, it is a necessity that to have been incorporated into DNA/RNA, the purine (adenine and guanine) and pyrimidine (cytosine, thymine, and uracil) nucleobases must have been readily available. Despite a significant research endeavor, terrestrial nucleobase origins are still unclear; also, it is unknown whether they were metabolized specifically for use in DNA/RNA or if they were simply part of the prebiotic organic inventory; if it is the latter case, it is essential to determine their formation and destruction mechanisms and subsequently how abundant they may have been on the primordial Earth.

The pioneering work of Miller (1953) provided the first evidence that complex organics (amino acids, sugars, and nu-

cleic acid precursors) could potentially be created by electric discharge in a primordial Earth-like environment and was the motivation for many successive experiments in the following decades. The synthesis of adenine ($C_5N_5H_5$; Figure 1) from concentrated ammonium cyanide solutions, heated to $80^\circ C$ – $90^\circ C$, was first demonstrated by Oró (1960) and Oró & Kimball (1962). Since then, numerous studies have reported nucleobase formation under various terrestrial conditions (Ponnampetuma et al. 1963; Levy & Miller 1999; Saladino et al. 2001; Hill & Orgel 2002; Borquez et al. 2005); however, due to low yields and susceptibility to hydrolysis (Shapiro 1995; Levy & Miller 1998), the accumulation of a large quantity of terrestrially synthesized nucleobases remains troublesome.

The organic inventory available on the early Earth was likely augmented by several exogenous sources (Greenberg 1989; Chyba 1990; Chyba et al. 1990), including atmospheric impact-shock synthesis (Bar-Nun et al. 1970; Fegley et al. 1986) and direct delivery of intact organics amidst comets, meteorites (Chyba et al. 1990), and interplanetary dust particles (IDPs; Anders 1989). Chyba & Sagan (1992) have compared the mass influx rate of organics by endogenous and exogenous sources, and report that for a presumably non-reducing terrestrial atmosphere ($[H_2]/[CO_2] \leq 0.1$) the influx of IDPs was the predominant source of prebiotic organics. It has been estimated that during the time period where life is thought to have begun—between 4.2 Gyr and 3.9 Gyr ago—up to 10^{20} g of intact organic material could have been brought to the Earth via IDPs (Brack 1999). A detailed investigation of how biologically important interstellar molecules may form, their rates of production, and their survival lifetimes must therefore be undertaken in an effort

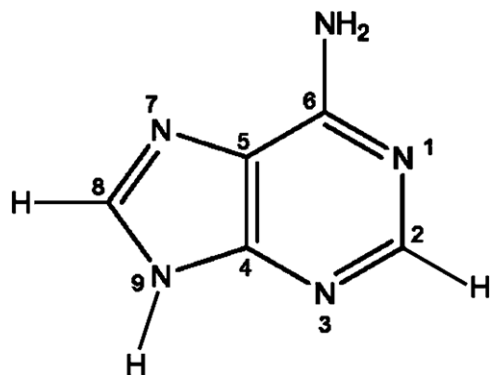


Figure 1. N(9)H tautomer of the nucleic acid base adenine ($C_5N_5H_5$).

to further understand the chemical environment on the prebiotic Earth.

Let us consider the formation of N-heterocyclic nucleobases, and more specifically adenine, in the interstellar medium (ISM). The synthesis of adenine via gas-phase pathways in diffuse molecular clouds by hydrogen cyanide (HCN) oligomerization has been suggested (Ghosh & Ghosh 1980; Chakrabarti & Chakrabarti 2000; Ehrenfreund & Charnley 2000; Glaser et al. 2007). However, the HCN dimerization rate (Smith et al. 2001), the inclusion of nitrogen into aromatic rings (Ricci et al. 2001), and the presence of large reaction barriers (Roy et al. 2007) are significant factors which may limit the gas-phase production of adenine within such environments. Astronomical observations (Charnley et al. 2001, 2005; Tielens 2008) have yet to identify adenine or its N-heterocyclic precursors in the gas phase.

It is perhaps more likely that adenine may form in the solid state either inside or on the surfaces of interstellar grains within molecular clouds. These small (up to a few 100 nm) icy grains exist at low temperatures, down to 10 K, and typically consist of a silicate/carbonaceous core covered with simple volatiles which have frozen out of the ISM—predominantly water (H_2O), but other detected species include carbon monoxide (CO), carbon dioxide (CO_2), ammonia (NH_3), methane (CH_4), formaldehyde (H_2CO), methanol (CH_3OH), and carbonyl sulfide (OCS) (Gibb et al. 2004). These molecules serve as precursor species to the formation of more complex species as these ices are known to be chemically processed by both the charged particle and ultraviolet (UV) photon components of the galactic cosmic radiation (GCR). Laboratory experiments studying these phenomena have shown that both amino acids and nucleobases are created by UV photolysis (Bernstein et al. 2002; Muñoz Caro et al. 2002; Simakov & Kuzicheva 2005; Nuevo et al. 2007, 2008, 2009), electron irradiation (Holtom et al. 2005; Cáceres et al. 2006; Lafosse et al. 2006), proton (H^+) irradiation (Kobayashi et al. 1995), and highly charged heavy-ion irradiation (Pilling et al. 2010) of interstellar ice analogs. In addition, much of the cosmic carbon ($\sim 20\%$) available to participate in adenine synthesis may already be incorporated into structurally similar species, such as polycyclic aromatic hydrocarbons (PAHs; Allamandola et al. 1989; Ehrenfreund & Charnley 2000), and N-heterocyclic PAHs (Mattioda et al. 2003), which are expected to be abundant within the ISM, and may also condense onto cold interstellar grains (Bernstein et al. 2005). Similarly, radiation-induced chemistry on these PAH-like grain surfaces and inside grain cavities is known to produce complex organics (Cecchi-Pestellini et al. 2004; Rimola & Ugliengo 2009) increasing the likelihood that grains are indeed a plausible location for interstellar nucleobases. In fact, there is evidence of

extraterrestrial biologically important molecules in meteorites (for a review, see Botta & Bada 2002) including the discovery of the nucleobase uracil within the Murchison meteorite (Martins et al. 2008).

However, in order to determine whether or not these molecules could have seeded the primordial Earth, we need to understand how likely it is that they could survive the harsh irradiation field experienced not only in the ISM, but also from the Sun within our solar system. The survivability of nucleobases and their precursors in interstellar ice analogs under UV radiation has been discussed previously (Peeters et al. 2003, 2005; Nuevo et al. 2009). The main conclusions drawn from this work are that (1) decay half-lives of cyclic molecules decrease with the number of nitrogen atoms in the ring, (2) nucleobase half-lives are short at 1 AU from the Sun (hr) or in diffuse clouds (yr) where they are unshielded from the UV radiation, and (3) half-lives are greatly increased (10^6 yr) in UV-shielded environments such as dense clouds (DCs). These findings cannot exclude the possibility that nucleobases formed in UV-shielded environments can survive over the lifetime of a typical dark cloud such as Taurus molecular cloud 1 (TMC-1). Dense molecular clouds and icy grain mantles serve to shield molecules from UV destruction, but do not shield from energetic charged particles of the GCR which are able to penetrate deep into these environments, and biomolecules which are formed here are subject to their destructive influence. Here, we report on the degradation rate of adenine ices at 10 K under simulated interstellar conditions in an attempt to estimate the survivability of this important biomolecule under radiation by the charged particle component of the GCR. In addition, data on the reaction of oxygen atoms with adenine in extraterrestrial icy grains are presented.

2. EXPERIMENT

The experiments were conducted using the surface scattering machine at the University of Hawaii (Bennett et al. 2004; Jamieson et al. 2006) which was modified to accommodate a biomolecule sublimation source. Within our main vacuum chamber, held at 8.0×10^{-11} torr, adenine powder (Sigma-Aldrich, purity $> 99\%$) is placed in a cylindrical stainless steel sample holder which is positioned 6 mm in front of a highly polished silver wafer maintained at 11.4 ± 0.3 K by a two-stage closed cycle helium refrigerator. The sample holder is surrounded by an oxygen-free high-conductivity (OFHC) copper cylinder to which a programmable 50 W cartridge heater and a silicon diode temperature sensor are attached. This oven is then heated to 443 K at ~ 1 K $minute^{-1}$ and is allowed to cool to 383 K during a 4 hr deposition process. During this time, the sublimating adenine molecules are deposited onto the cooled silver target. To determine the ice thickness, the column density, N , in molecules cm^{-2} , is calculated according to Bennett et al. (2004). It is acknowledged that the validity of using this technique has recently been brought into question due to the presence of optical interference (e.g., Teolis et al. 2007); however, it should be stressed that deviations caused by fringing are only observed for thick ices (typically $> 1 \mu m$) and in addition, these interference effects are wavelength dependent. Thus, deviations can be suppressed by calculating the average thickness as determined from individual bands over a range of the spectrum; here, 17 bands between 750 and 1750 cm^{-1} (see Table 1) were chosen. The absorption intensity in cm^{-1} is obtained by taking the area under a Gaussian fit of each spectral feature, and the frequency-dependent absorption coefficients are taken from the theoretical B3LYP/6-31G(d,p) values of Nowak

Table 1
Infrared Absorptions of Adenine Ice at 10 K Prior to Irradiation, Along with the Corresponding Assignments of the Observed Bands

Frequency (cm ⁻¹)	Frequency ^a (cm ⁻¹)	Mode ^b	Characterization ^b
1681	1639, 1633	ν_6	β NH ₂ scis (28), ν C6N10 (21), ν C5C6 (19)
1609	1612	ν_7	ν N3C4 (27), ν C5C6 (12)
1506		ν_8	β NH ₂ (48), ν C4C5 (12)
1456	1474	ν_{10}	ν C6N1 (24), β C2H (27), ν C6N10 (13), β NH ₂ scis (12), ν C2N3 (12)
1420	1419	ν_{11}	ν C4C5 (27), ν C4N9 (21)
1368	1345	ν_{13}	ν N9C8 (20), β C8H (13), β N9H (10), ν C6N1 (10)
1335	1328	ν_{14}	ν N1C2 (31), ν C5N7 (19), β C2H (11)
1309	1290	ν_{15}	ν C2N3 (43), ν C5N7 (13), ν N1C2 (10)
1255	1240	ν_{16}	β C8H (36), ν N7C8 (16), β N9H (10)
1160	1229	ν_{17}	β NH ₂ rock (26), ν C5N7 (22)
1126	1127	ν_{18}	ν C4N9 (20), β r4 (10), ν C6N10 (10)
1021	1061, 1032	ν_{19}	ν C8N9 (55), β N9H (32)
944	927	ν_{22}	β r4 (42), β r5 (32), ν C4C5 (11)
914	887	ν_{23}	β R1 (49), β R3 (15)
850	848	ν_{24}	γ C8H (90)
800	802	ν_{25}	τ R1 (46), τ r4 (20), γ C6N10 (19), γ C8H (15)
723	717	ν_{26}	ν N3C4 (20), β r4 (14), ν C5N7 (11), ν C4N9 (10)

Notes.

^a Values taken from Ar matrix isolation experiments of Nowak et al. (1996).

^b Assignments taken from B3LYP/6–31 G(d,p) calculations of Nowak et al. (1996).

et al. (1996); to our knowledge no experimental values have been taken in the solid state. Using this method, we determine the pre-irradiation column density, $N_o = (8.10 \pm 0.76) \times 10^{16}$ molecules cm⁻², and the ice thickness, $d = N_o M / N_A \rho = 130 \pm 14$ nm; here, $M = 135.1$ amu and $\rho = 1.49$ g cm⁻³ (Kilday 1978) are the molecular mass and density of adenine, respectively, and N_A is Avogadro's number.

Test experiments determined that the close proximity of the oven to the silver wafer does not increase the wafer temperature and that adenine vapor condenses on the silver wafer only at oven temperatures above 403 K. This assures that no sample decomposition occurs during the deposition sequence. Note that in order to remove the water being deposited in our ice, which could serve as a potential contaminant during the experiment, the adenine sample was located inside the vacuum chamber during the bake-out procedure of the vessel, whereby it was typically held for 36 hr at 343 K; this temperature is below the reported sublimation temperature of adenine (Nowak et al. 1996; Glavin et al. 2002; Jochims et al. 2005). Previous experiments (Satzger et al. 2006; Evans & Ullrich 2010) have verified that thermal decomposition is negligible at the sublimation temperatures used here; further, the N(9)–H tautomer is the dominant species in the gas phase (Lin et al. 1980; Brown et al. 1989).

Besides the pure adenine samples, some early work has also been carried out to investigate how oxygen atoms formed upon irradiation may interact with adenine, whereby a 500 nm thick layer of molecular oxygen (O₂) is condensed on top of both a neat adenine ice and one which had already undergone the standard irradiation sequence. A secondary deposition arm was used to condense the molecular oxygen (99.998%; GasPro) layer in order to prevent thermal reactions with the adenine, which remains hot in the sample oven. While it is likely that adenine may form within the polar regions of an astronomical ice which is dominated by water ice, this oxygen-covered adenine ice is still interesting to investigate for the following reasons: (1) in DCs where the temperature is low, the outer layers of astronomical ices are expected to be apolar in nature, consisting primarily of O₂, but also CO, and molecular nitrogen (N₂) and would partly act as a shield for the interior of the

ices (particularly from UV photons; Ehrenfreund et al. 1992), (2) there are many oxygen-bearing species (such as H₂O, O₂, CO, CO₂) within the polar regions of astronomical ices which, when exposed to the GRC, can yield atomic oxygen (Bennett & Kaiser 2005; Loeffler et al. 2006; Zheng et al. 2006; Teolis et al. 2009), and (3) considering that adenine (C₅N₅H₅) contains no oxygen itself, we are here uniquely able to easily identify (via the appearance of new infrared absorptions characteristic of C–O, N–O, and O–H bonds) and effectively isolate interactions occurring between the O₂ matrix and adenine. Oxygen then serves as a model compound and allows one to speculate what products may arise were a different matrix/reactant present.

The standard irradiation procedure is as follows. All neat adenine samples are irradiated for 3 hr with 5 keV electrons emitted from an SPECS model EQ 22–35 electron gun operating at a filament current of 1 μ A. All oxygen-covered adenine samples were irradiated for 2 hr with electron energy and current identical to the neat adenine experiment. The EQ 22–35 has a 78.8% extraction efficiency and scans the electrons over a 3.2 ± 0.3 cm² surface of the silver wafer; the electron flux is then, $\phi = 1.54 \times 10^{12}$ electrons cm⁻² s⁻¹. The chemical processing of the adenine ices is monitored on line and in situ by a Thermolectron 6700 FTIR (Fourier Transform Infrared) spectrometer. Spectra (194 scans from 6000 to 400 cm⁻¹ at 2 cm⁻¹ resolution) are continuously recorded during irradiation in 1.6 minute intervals. After being held isothermally at 11 K without further irradiation for 30 minutes, the samples are heated to room temperature at a rate of 0.5 K minute⁻¹.

3. RESULTS

The infrared spectrum over the range of 4000–500 cm⁻¹ of the adenine ice prior to irradiation is shown in Figure 2 (black line); mode assignments are taken from the argon matrix isolation experiments of Nowak et al. (1996) and are listed in Table 1. Large frequency shifts, up to 60 cm⁻¹, are seen for the ν_6 , ν_{10} , ν_{13} , ν_{17} , ν_{19} , and ν_{23} modes; all of these involve hydrogen (H) atom or amino group (NH₂) motion. These shifts are caused by intermolecular adenine–adenine interactions, which

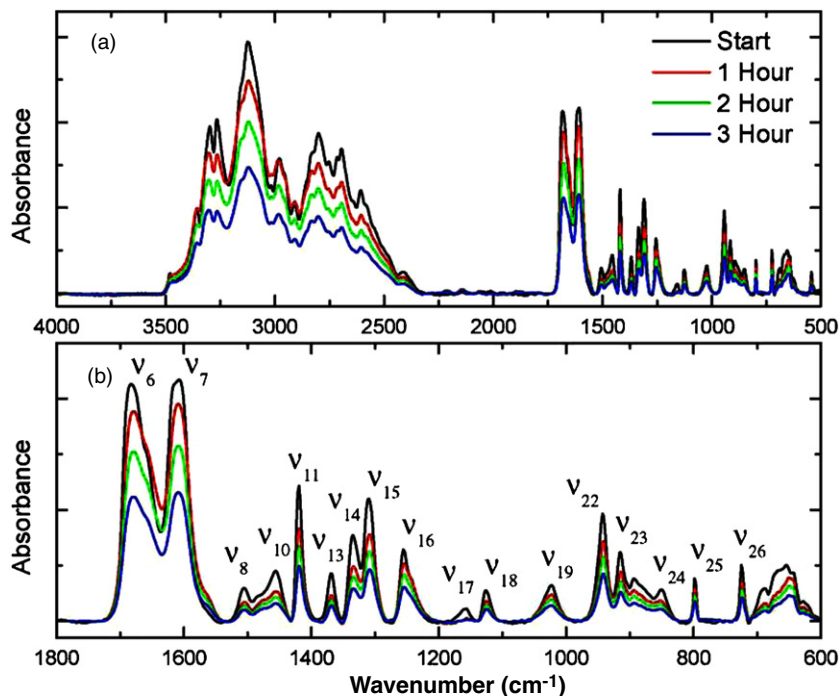


Figure 2. FTIR spectra: (a) 4000–500 cm^{-1} and (b) 1800–600 cm^{-1} of adenine at 11 K in 1 hr intervals of electron irradiation. Mode assignments from Nowak et al. 1996 are shown in panel (b). Characteristic ν_{11} , ν_{14} , ν_{16} , and ν_{25} modes are utilized to extract decay constants.

(A color version of this figure is available in the online journal.)

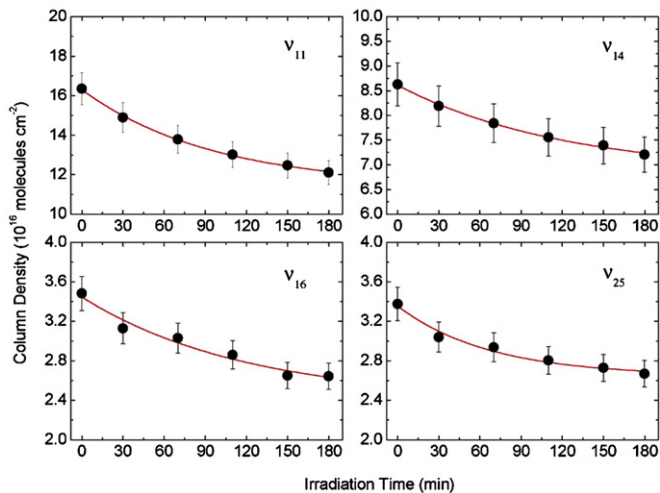


Figure 3. Calculated column densities of the ν_{11} , ν_{14} , ν_{16} , and ν_{25} modes plotted vs. irradiation time. Fits shown in red are used to determine the half-life of adenine under cosmic proton flux; see the text for a detailed discussion.

(A color version of this figure is available in the online journal.)

are absent in the argon matrix isolation experiments. Apart from these shifts, our peak positions agree exceptionally well with the matrix isolation studies. Upon electron irradiation, the absorption intensity decreases by at least 25% for all modes as can be visualized in Figure 2. The absorption intensity of several prominent modes, including ν_{11} , ν_{14} , ν_{16} , and ν_{25} , is monitored throughout the irradiation in order to quantify the decomposition kinetics of the adenine ice. Column densities for each characteristic mode are calculated according to Bennett et al. (2004) and are plotted versus irradiation time in Figure 3. These data are fit with a unimolecular decomposition of the adenine via (pseudo) first-order kinetics (Steinfeld et al. 1999)

as quantified via Equation (1):

$$N(t) = N_0 e^{-k_i t}, \quad (1)$$

with $N(t)$ being the column density at a time t , N_0 the initial column density, and k_i is the decay constant of the i th mode. These fits yield the decay parameters (in s^{-1}) of $k_1 = (1.48 \pm 0.14) \times 10^{-4}$, $k_2 = (1.51 \pm 0.25) \times 10^{-4}$, $k_3 = (1.40 \pm 0.37) \times 10^{-4}$, and $k_4 = (2.21 \pm 0.71) \times 10^{-4}$ for the ν_{11} , ν_{14} , ν_{16} , and ν_{25} modes, respectively. From these values, the average decay constant, $k_a = (1.65 \pm 0.37) \times 10^{-4} \text{ s}^{-1}$, is obtained for use in subsequent calculations.

The solid state and gas-phase decomposition of adenine may be expected to proceed by similar mechanisms. In the gas phase, mass spectroscopy has identified the loss of successive hydrogen cyanide or hydrogen isocyanide (HNC) units as the main fragmentation pathway for several irradiation sources including 70 eV electrons (Rice & Dudek 1967), 6–22 eV photons (Jochims et al. 2005), 56 keV Ar^{8+} ions (Martin et al. 2008), and 3 keV Cl^+ ions (Bredy et al. 2009). However, absorption lines of HCN/HNC could not be observed due to the complexity of the adenine parent spectrum. The ν_1 C–H stretch of HCN at 3306 cm^{-1} (Satoshi et al. 1997) and the ν_1 N–H stretch of HNC at 3620 cm^{-1} (Milligan & Jacox 1967) are not observed as they arise in a region where severe spectral broadening is present due to interactions between neighboring adenine molecules. The ν_2 bending mode of HCN at 721 cm^{-1} (Satoshi et al. 1997) is not detected due to overlap with the ν_{26} mode of adenine. The ν_2 bending mode of HNC at 477 cm^{-1} (Milligan & Jacox 1967) is at the edge of the FTIR detection range and could not be resolved due to poor signal-to-noise ratios. The ν_3 C \equiv N stretch of HCN at 2098 cm^{-1} (Satoshi et al. 1997) and the ν_3 C = N stretch of HNC at 2029 cm^{-1} (Milligan & Jacox 1967) are in a region where the adenine spectrum is featureless, but both of these modes are very weak in absorption.

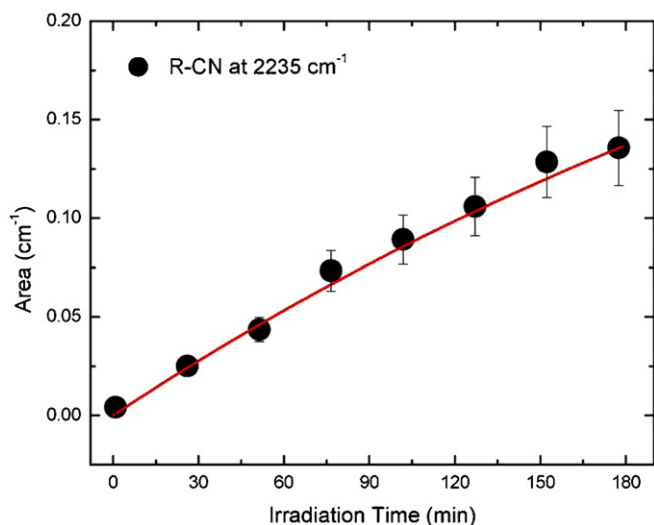


Figure 4. Absorption intensity rise profile and first-order fit of R-C≡N peak seen at 2235 cm⁻¹ during neat adenine irradiation.

(A color version of this figure is available in the online journal.)

While HCN/HNC absorptions are not visible in our spectrum we do see evidence of one novel band at 2235 cm⁻¹ which arises during neat adenine irradiation and is assigned as an R-C≡N mode (Socrates 2001). The saturated heterocyclic adenine parent will inevitably produce unsaturated bonds after electron impact fragmentation, and CN radicals within our ice are able to bond at these positions to yield the R-C≡N product. This mechanism for R-C≡N production is adopted based on previous experimental work involving cyano radical reactions with unsaturated compounds (acetylene, ethylene, methylacetylene, allene, dimethylacetylene, benzene) similar to adenine (Balucani et al. 2000), as well as propylene (Gu et al. 2008), and diacetylene (Zhang et al. 2009), whereby the nearly barrier-less addition of the cyano radical to these unsaturated species is reported. The band at 2235 cm⁻¹ displays a first-order rise profile, which is plotted as a function of irradiation time in Figure 4 along with a first-order fit (see Equation (1));

this yields a production rate for the R-C≡N feature of $4.53 \pm 0.58 \times 10^{-5} \text{ s}^{-1}$.

We would now like to briefly address the irradiation of both the neat and pre-irradiated oxygen-covered adenine ices. Upon electron irradiation of all oxygen-covered ices, less than 3% degradation of the characteristic adenine bands is observed, and column density decay profiles could not be extracted for comparison to the pure adenine irradiation experiments. However, based on the initial and final absorption strengths, the decay constant for oxygen-covered adenine can roughly be estimated to be two orders of magnitude smaller than was established for the pure adenine ice—indicative of the protection afforded by the layer of molecular oxygen and supporting the capability of such a layer protecting molecular species within interstellar grains. In both experiments, the formation of ozone (O₃) was observed upon the onset of electron irradiation as evidenced by the appearance of absorption bands at 702 (ν₂), 1035 (ν₃), and 2108 (ν₁+ν₃) cm⁻¹; this serves as confirmation that energetic electrons are interacting with O₂ on the adenine ice, which dissociate into atomic oxygen, and subsequently react with molecular oxygen forming ozone (Bennett & Kaiser 2005). The R-C≡N mode at 2235 cm⁻¹ seen during the irradiation of pure adenine is also observed here. Additional absorption features unique to this experiment arise at 1871, 1750, 1610, 1242, and 737 cm⁻¹. These features are stronger in the pre-irradiated oxygen-covered adenine ice experiment and are presented in Figure 5. As these absorption bands were not identified within irradiated ices of pure adenine, or pure molecular oxygen, we associate them with oxygen-bearing species formed as a result of reactions between these two ice components. The absorption of all oxygen-bearing products is seen in Figure 6 to be very distinct from the temporal profiles of ozone, and R-C≡N (Figure 4). Here, the profiles of the oxygen-bearing species rise very slowly initially during the irradiation; after approximately 75 minutes, a steeper rise is observed in the profiles. Note that the oxygen atoms necessary for the chemical reaction are formed via unimolecular decomposition of O₂ (Bennett & Kaiser 2005), which is deposited on top of the adenine layer. Therefore, the locations of the oxygen source and oxygen sinks are spatially separated. Consequently, we attribute

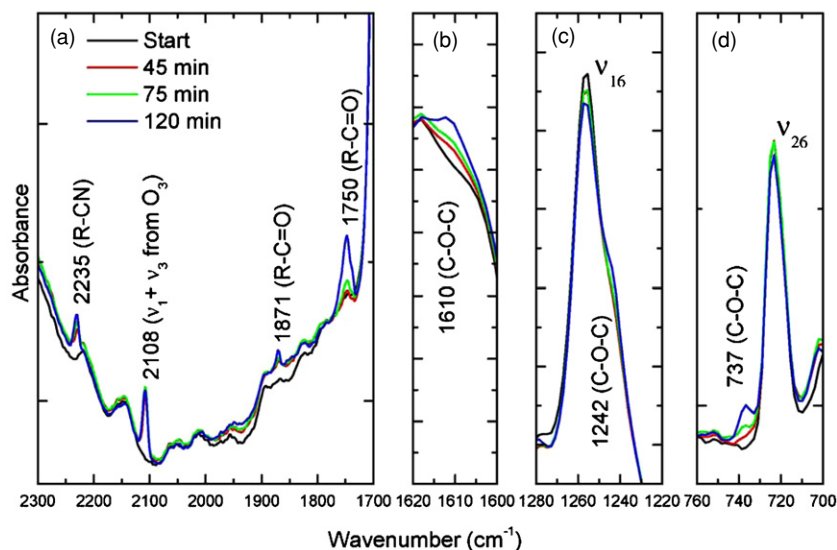


Figure 5. FTIR spectra (a) 2300–1700 cm⁻¹, (b) 1620–1600 cm⁻¹, (c) 1280–1220 cm⁻¹, and (d) 760–700 cm⁻¹ of pre-irradiated oxygen-covered adenine at 11 K during electron irradiation at 5 keV. Assignment of ozone is taken from Bennett et al. (2005); assignment of other bands from Socrates (2001).

(A color version of this figure is available in the online journal.)

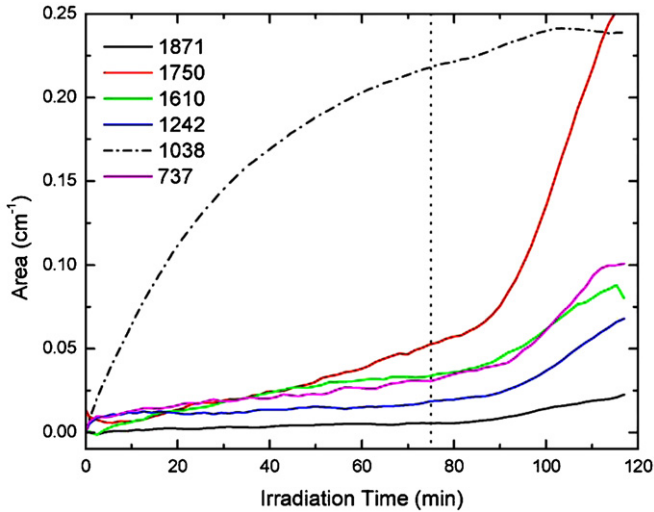


Figure 6. Absorption intensity rise profiles of oxygen-bearing products seen during oxygen-covered pre-irradiated adenine ice irradiation. Product species are identified as follows: R-C=O (carbonyl group) at 1871 (black) and 1750 (red) cm^{-1} ; C-O-C (epoxide) at 1610 (green), 1242 (blue), and 737 (magenta) cm^{-1} ; ozone at 1038 (dashed) cm^{-1} . The vertical dotted line indicates the beginning of oxygen atom interaction with adenine.

(A color version of this figure is available in the online journal.)

this time delay to the time needed for oxygen atoms to diffuse through the O_2 layer before reaching the adenine ice. Note that these oxygen atoms can be generated with excess energy of a few eV from molecular oxygen (Cosby 1993); this excess energy helps to overcome the “activation energy” necessary to diffuse through the ice, but also to react with the adenine molecule. The bands at 1871 and 1750 cm^{-1} are characteristic of a CO stretch, indicating the formation of a carbonyl group (C=O; Socrates 2001). We are also able to determine the formation of epoxides as evidenced by the bands at 737 (asymmetric C-O-C ring breathing), 1242 (symmetric C-O-C ring breathing), and 1610 cm^{-1} (aromatic ring buckling; Hawkins & Andrews 1983; Tait et al. 1995; Socrates 2001; Bennett et al. 2005; Liu et al. 2005).

4. DISCUSSION

The discussion is divided into two parts. First, the destruction of the adenine molecule is quantified and its half-life is determined within several different interstellar environments (Section 4.1). Second, the formation of new molecules (nitriles, epoxides, carbonyl functions) within the ice is investigated, and reaction mechanisms are proposed (Section 4.2).

4.1. Destruction of Adenine

It is important to stress that our experiments monitored the destruction of adenine by energetic electrons; our kinetic analysis suggests decay rates of $k_a = (1.65 \pm 0.37) \times 10^{-4} \text{ s}^{-1}$ for pure adenine ices (recall that it was not possible to determine reliable decay parameters for the O_2 -covered ices, so subsequent calculations of half-lives will be based on this value). It is important to transfer these findings to “real” astrobiologically relevant environments. This is addressed by quantifying the survivability of adenine within the solar system and in several interstellar environments by calculating the half-life using a similar approach to that carried out by Peeters et al. (2003).

First, we calculate the electron destruction cross section of a single electron passing through our ice, whereby, $\sigma =$

$(1.07 \pm 0.24) \times 10^{-16} \text{ cm}^2$, according to $\sigma = k_a/\varphi$, where $\varphi = 1.54 \times 10^{12} \text{ electrons cm}^{-2} \text{ s}^{-1}$ is the laboratory electron flux and k_a is the average decay parameter derived in Section 3. The stated error results from uncertainties in fitting the decay parameter. It is noted that the destructive cross sections for keV electrons refer to inelastic scattering processes. Experimentally determined cross section data in this energy range are scarce, as noted by Blanco & García (2007), who calculated the inelastic cross section for scattering of 5 keV electrons from gaseous adenine using the screening-corrected additivity rule (SCAR) and reported the value $\sigma_{\text{in}} = 1.67 \times 10^{-16} \text{ cm}^2$. However, two related experimental studies of interest are mentioned here. Isaacson (1972) measured the inelastic scattering of 25 keV electrons from gaseous adenine and found a cross section of $\sigma_{\text{in}} = 3.6 \times 10^{-17} \text{ cm}^2$, and total dissociative cross sections on the order of 10^{-17} cm^2 are reported for scattering of low-energy electrons (a few eV) from thin films of adenine (Panajotović et al. 2007). Our electron destruction cross section results are in general agreement with these findings.

It is necessary to scale the calculated electron destruction cross section of our keV electrons to an *effective* destruction cross section for the MeV proton component of the GCR. The validity of simulating proton irradiation with keV electron impact has been discussed in detail previously (Kaiser et al. 1997; Kaiser & Roessler 1998; Jamieson et al. 2006; Bennett et al. 2009) and is based on calculations of energy loss mechanisms as protons and electrons pass through a solid. The linear energy transfer (LET) is a measure of the energy deposited into a material per unit distance as energetic particles travel through it, and is used here to quantify the destructive effect of ionizing radiation. Ion trajectory simulations using the SRIM/TRIM code (Ziegler et al. 1985) reveal that the LET_{H^+} of 0.001, 1.0, and 10 MeV protons in solid adenine is 21.9, 34.8, and 6.4 keV μm^{-1} , with 85.6%, 99.9%, and 99.9% of this energy loss proceeding through inelastic electronic interactions with the target molecules, respectively; this leads to electronic excited states of the molecules, unimolecular decomposition, and/or free secondary electrons. Secondary electrons are generated with energies up to a few keV (Magee & Chatterjee 1987) and are therefore directly modeled by our radiation source. The LET_e of a 5 keV electron as it traverses our ice is calculated to be 3.62 keV μm^{-1} using the CASINO code (Drouin et al. 2007). Therefore, the LET of a single electron does not directly translate to the same radiation damage caused by a single proton, so electron destruction cross sections are scaled by the ratio ($\text{LET}_{\text{H}^+}/\text{LET}_e$) to give an *effective* destruction cross section, σ_{eff} , which more accurately models damage from protons at particular energies; results are summarized in Table 2. An advantage of employing this scaling method is that it allows simulation of the dominating inelastic electronic transfer processes of protons at multiple energies with a monoenergetic electron source.

In order to determine the cosmic survivability of adenine in astrobiologically relevant radiation environments, the decay half-life is calculated according to Equation (2):

$$t_{1/2} = \ln(2)/\sigma_{\text{eff}}\varphi_p, \quad (2)$$

where σ_{eff} is the *effective* electron destruction cross section and φ_p is the proton flux in each specific environment. In this scenario, it is assumed that a given amount of adenine is initially present and that no additional production pathways are present. Thus, given the reported flux of protons within a particular astronomical environment, which are taken as the values reported by Palumbo et al. (2008), we are able to

Table 2
Calculated Half-lives of Adenine within our Solar System (at Distances of 1 and 40 AU), as well as in the Interstellar Medium (DC: Dense Clouds, DISM: Diffuse Interstellar Medium)^a

Radiation Source	σ_{eff} (cm ² per molecule)	Flux				Half-life			
		1 AU (cm ⁻² s ⁻¹)	40 AU (cm ⁻² s ⁻¹)	DC (cm ⁻² s ⁻¹)	DISM (cm ⁻² s ⁻¹)	1 AU (s)	40 AU (yr)	DC (Myr)	DISM (Myr)
1 MeV H ⁺	1.03×10^{-15} ^b	3.3×10^2 ^c	2.1×10^{-1} ^d	1.0 ^c	1.8 ^c	2.04×10^{12}	1.02×10^8	21.3	11.9
1 keV H ⁺	6.48×10^{-16} ^b	3.0×10^8 ^c	1.9×10^5 ^d	-	-	3.57×10^6	1.79×10^2	-	-
UV ^e	2.7×10^{-18}	3.0×10^{13}	1.9×10^{10} ^d	1.0×10^3	1.0×10^8	8.65×10^3	4.28×10^{-1} ^d	8.27	8.27×10^{-5}
Total	-	-	-	-	-	8.63×10^3	4.27×10^{-1}	5.97	8.27×10^{-5}

Notes.

^a Also shown are the effective destruction cross sections (σ_{eff}), and the relevant fluxes of each irradiation source in each astrophysical environment.

^b Effective cross sections calculated by scaling the 5 keV electron destruction cross section by the energy loss ratio ($\text{LET}_{\text{H}^+}/\text{LET}_e$).

^c Combined contribution from GCRs and solar flares estimated from Palumbo et al. (2008).

^d Scaled from the value at 1 AU, using $1/r^2$ at a distance of 40 AU for a typical Kuiper Belt object.

^e Values taken from Peeters et al. (2003).

estimate the half-life of adenine. At a distance of 1 AU the flux for 1 keV H⁺ nuclei from the solar wind is given as $\varphi_p = 3.0 \times 10^8$ cm⁻² s⁻¹; combined with an averaged flux of 1 MeV H⁺ nuclei from solar flares is given as $\varphi_p = 3.2 \times 10^2$ cm⁻² s⁻¹. The contribution from GCRs adds a further $\varphi_p = 1.0 \times 10^1$ cm⁻² s⁻¹ of 1 MeV H⁺ nuclei. Meanwhile, at a distance of 40 AU—a typical orbital distance for a Kuiper Belt object—the contribution from GCRs is unchanged, but all other values are scaled by the relationship r^{-2} . Considering next the interstellar environments, we adopt values of $\varphi_p = 1.8$ cm⁻² s⁻¹ of 1 MeV H⁺ nuclei and $\varphi_{\text{uv}} = 1.0 \times 10^8$ cm⁻² s⁻¹ for the diffuse ISM (DISM; where visual extinction $A_v \leq 1$ mag) and $\varphi_p = 1.0$ cm⁻² s⁻¹ of 1 MeV H⁺ nuclei and $\varphi_{\text{uv}} = 1.0 \times 10^3$ cm⁻² s⁻¹ for DCs ($A_v > 5$ mag). The half-life of adenine in each environment due to the individual proton destruction processes is calculated and reported in Table 2. However, molecules in the ISM are subject to destruction by both H⁺ and UV irradiation, and discussions of cosmic survivability must consider both processes; we take UV half-lives as reported by Peeters et al. (2003). The *total* half-life of adenine is calculated according to Equation (3) where destruction due to UV photons, 1 keV H⁺ and 1 MeV H⁺ nuclei are treated as three independent processes:

$$\frac{1}{T_{1/2}} = \sum_i \frac{1}{t_i}, \quad (3)$$

where $T_{1/2}$ is the *total* half-life and t_i is the half-life due to the *i*th destruction process. *Effective* cross sections, fluxes, individually calculated half-lives from each contributing radiation source, as well as the *total* half-lives, are compiled in Table 2 for each astronomical environment considered here.

Half-lives within the solar system at 1 AU and 40 AU from the Sun are essentially determined by the UV flux within these environments; inclusion of the additional proton-induced destruction rates reduces the lifetime of adenine by only 0.29% and 0.24%, respectively. While the decreased UV flux at 40 AU does enhance the expected half-life of adenine by a factor of 1.56×10^3 , it is still relatively short on astronomical timescales, and the survivability of unshielded adenine remains unlikely. A similar situation is found for the DISM, where the photon flux is found to be eight orders of magnitude larger than the proton flux, leading to a half-life of 82.7 yr—the same value as reported when UV radiation alone is taken into account (Peeters et al. 2003). However, in a DC, the UV flux can be attenuated by a factor of up to 10^5 (Prasad & Tarafdar 1983), and it is here that the destruction of adenine by MeV protons

becomes significant. Indeed, the proton (21.3 Myr) and UV (8.2 Myr) half-lives are within a factor of ~ 3 , and the total half-life (5.9 Myr) is $\sim 30\%$ shorter than the UV-only half-life. Of significant astrobiological interest is the fact that while our result decreases the overall lifetime of adenine in DCs it does not exclude the possibility that adenine should remain relatively abundant over the lifetime of typical molecular clouds. As an example, let us consider the case of the cold, dense interstellar cloud TMC-1, which is estimated to be 6 Myr old (Cohen & Kuhl 1979). Assuming uniform UV shielding throughout the cloud, one would expect 50% of the initially available adenine to still be present. This result is valid within our initial assumption that adenine begins at some initial concentration and is subsequently degraded by both UV photons and energetic particles without accompanying production mechanisms, which is of course an over-simplification of the realistic scenario. In fact, these irradiation sources are likely to also be processing these ices and contributing to the production of adenine within these ices, as adenine has been observed to form within irradiated ices in laboratory experiments simulating these environments (see Section 1). It is likely that both production and destruction mechanisms for adenine are in competition with one another; it is anticipated that a steady-state abundance of adenine will be reached for each particular astronomical environment.

4.2. Formation of New Products

Having commented on the destruction rates of adenine, we are now discussing possible reaction products, i.e., the spectroscopically detected nitriles, epoxides, and carbonyl functions evident upon irradiation of adenine and oxygen ices. In pure adenine ices, it is important to note that the destruction rate of the adenine ($(1.65 \pm 0.37) \times 10^{-4}$ s⁻¹) is—within the error limits—a factor of about three higher than the production rate of R-C≡N ($(0.45 \pm 0.06) \times 10^{-4}$ s⁻¹), and also, that nitriles were the only new reaction product formed in the solid state. On the other hand, as discussed, gas-phase studies provide compelling evidence for the formation of HCN/HNC (Rice & Dudek 1967; Jochims et al. 2005; Martin et al. 2008; Bredy et al. 2009). How can these results be combined into a coherent picture? We propose that in the solid state, a unimolecular decomposition of adenine leads to the formation of CN radicals; the formation of radicals in the unimolecular decomposition of organic molecules with energetic electrons is well established, for instance, in the formation of CH₃O and CH₂OH radicals in the decomposition of methanol (CH₃OH; Bennett et al. 2007). The cyano radical

can react within a matrix cage to add without barrier to the aromatic adenine molecule across either a carbon or nitrogen atom leading to the formation of a generic doublet radical intermediate; it is not feasible to assign the exact location to which the cyano radical adds since the reaction is not conducted under single collision conditions as in crossed beam experiments (Kaiser et al. 1998). Nevertheless, it is conceivable that this newly formed doublet radical can either (1) react with hydrogen atoms in the ice to form a closed shell nitrile, or (2) if there is an H atom bound to the carbon atom which is attacked by the cyano radical—such as at the C2 and C8 positions of adenine—it could also be possible for this hydrogen atom to be emitted during the process thus maintaining the aromaticity of the molecule; this in turn also forms a closed shell nitrile whereby a hydrogen atom was replaced by a CN group. Note that the interaction of energetic electrons with any organic molecule, such as methanol (Bennett et al. 2007), methane (Bennett et al. 2006), ethane (Kim et al. 2010), and methylamine (Holtom et al. 2005), leads to the formation of mobile hydrogen atoms in the solid ices even at 10 K—so does adenine. In this proposed mechanism, one adenine molecule is consumed by unimolecular decomposition forming the cyano radical, whereas this radical adds to the π system of a second adenine molecule. So in total, we would expect—if the formation of the nitriles is the only reactive pathway—that the decay rate constant is a factor of two higher than the rate constant associated with the formation of the nitrile. A comparison of these rate constants of $(1.65 \pm 0.37) \times 10^{-4} \text{ s}^{-1}$ versus $(0.45 \pm 0.06) \times 10^{-4} \text{ s}^{-1}$ shows that this tendency is actually observed.

We are turning our attention now to the oxygen-bearing molecular products. It is expected that suprathreshold oxygen atoms liberated from the dissociation of molecular oxygen—which are electrophilic—can add to the π electron density of the aromatic adenine molecule; similar processes have previously been observed for benzene. Here, the reactions have been studied in the gas-phase at room temperature and up to 1000 K, where oxygen atoms were generated by photolysis of nitrous oxide (N_2O ; Boocock & Cvetanović 1961; Taatjes et al. 2010), and within argon matrices held at 12 K where oxygen atoms were produced from the photolysis of O_3 (Parker & Davis 1999). In these studies, a wide range of products were observed including alcohols (phenol); epoxides (benzene oxide, which may isomerize to oxepin, where the oxygen is formally incorporated into the ring structure); ketones (2,4-cyclohexadienone); ketenes (hexa-1,3,5-trien-1-one); and the formation of five-membered rings (cyclopentadiene), which is accompanied by the evolution of gaseous carbon monoxide; infrared vibrational analysis additionally supports the production of aldehydes. More specifically, our studies indicate that we observe the presence of an epoxide group, as evidenced by infrared bands appearing at 737 (asymmetric C–O–C ring breathing), 1242 (symmetric C–O–C ring breathing), and 1610 cm^{-1} (aromatic ring buckling; Hawkins & Andrews 1983; Tait et al. 1995; Socrates 2001; Bennett et al. 2005; Liu et al. 2005; Figure 5). The epoxide formation is explained by the initial addition of an oxygen atom to a carbon atom leading to an O–C_a–C_b diradical which can then ring-close to form the epoxide; this can likely occur across the C4–C5 and/or C5–C6 atoms. Second, the features at 1871 and 1750 cm^{-1} are characteristic of the formation of a carbonyl group. While previous studies on benzene have led to the possibility of ring-opening reactions, we also consider what may happen if the oxygen atom again attacks a carbon atom with hydrogen bound to it (i.e., C_a is C2 or C8); here, in both cases the migration of

the hydrogen atom from C_a to the adjacent atom (which may be carbon or nitrogen) would yield a ketone structure. Indeed, there are studies to suggest that the C8 oxidation of adenine can occur readily (Gu et al. 2000). The formation of both epoxides and carbonyls has been demonstrated previously in low-temperature irradiation experiments; for example, the reaction of ethylene (C_2H_4) with oxygen atoms produced from both ozone (Hawkins & Andrews 1983) and carbon dioxide (Bennett et al. 2005) leads to the formation of both ethylene oxide ($\text{c-C}_2\text{H}_4\text{O}$) and acetaldehyde (CH_3CHO). These studies support our proposed reaction mechanisms.

5. ASTROPHYSICAL IMPLICATIONS

The nucleic acid base molecule adenine is thought to be synthesized from readily available molecules in the ISM by both gas-phase processes, and in the solid state on icy grains, initiated by the UV and charged particle component of the GCR. This radiation will simultaneously act to degrade adenine, and the competition between synthesis and degradation rates is expected to afford some steady-state abundance within astronomical environments. Destruction due to UV photons and charged particles in the GCR must both be considered; here, results on the destruction rate of adenine by simulated proton irradiation are presented and combined with previously reported UV destruction rates in an effort to determine the overall survivability of this important terrestrial biomolecule. Our discussion has neglected the competing formation rates and therefore the abundances we predict are likely to be underestimated.

Within our solar system, the half-life of adenine, due to proton and UV irradiation, is less than 0.5 yr. Due to such short half-lives predicted at 1 AU (Table 2), or even at 40 AU, how could adenine and other complex biomolecules have survived to seed the early Earth? In their study of the UV destruction of adenine, Peeters et al. (2003) also investigated the lifetime of the amino acid glycine, and found the lifetime to be a factor of 4.5 times lower than that of adenine meaning that the survival of this species over the age of our system would be even more unlikely. It is surprising then that the analysis of comet-exposed materials from NASA's stardust mission—obtained when it flew within 234 km of the surface of comet 81P/Wild 2—found that traces of glycine were present (Brownlee et al. 2004; Elsila et al. 2009). The comet itself has a volume of nearly 75 km^3 and is believed to have had a stable orbit within the Kuiper Belt ($\sim 40 \text{ AU}$) since the birth of the solar system. An encounter with Jupiter in 1974 has disturbed its orbit, bringing it into a dynamic orbit within the inner solar system, whereby it orbits roughly once every six years passing as close as 1.86 AU from the Sun (Sekanina & Yeomans 1985; Brownlee et al. 2006). An orbit so close to the Sun has caused the surface of the comet to become active; the additional heating causes the sublimation of volatiles. The outer layers of the comet began sublimating in the few hours prior to the Stardust flyby, and collected materials are thought to be from the interior of the comet, the pristine material that the solar system was formed from. The outer layers of the comet were able to sufficiently shield the fragile glycine molecule from the harsh irradiation environment of our solar system over the 4.5 billion years since its formation.

The penetration depth for both UV photons, as well as charged particles, is highly dependent upon the energy. Orzechowska et al. (2007) carried out an in-depth study of the UV photolysis of amino acids embedded within an H_2O ice matrix at 100 K, and found that the penetration depth of UV photons within water ice is $\sim 1 \mu\text{m}$ at 163 nm (7.6 eV), $\sim 1 \text{ cm}$ at 180 nm (6.9 eV), and

up to 1 m at 200–300 nm (4.1–6.2 eV). The half-life of glycine, isolated in water ice only 1.6 mm thick, was found to increase by two orders over the unshielded half-life of around 0.5 hr determined by Peeters et al. (2003). Using the SRIM/TRIM code, the calculated penetration depth for protons in water ice is again energy dependent whereby 1 keV H^+ nuclei penetrate only ~ 34 nm, 1 MeV H^+ nuclei are able to penetrate $\sim 18 \mu\text{m}$, and very high energy 1 GeV H^+ nuclei can penetrate around 3.2 m. Thus, just the few outer meters of any icy solar system body, such as a comet, should provide satisfactory shielding for the survival of large amounts of complex biomolecules.

In our solar system and in the DISM, the UV destruction rate dominates; the half-life is on the order of years, and accumulation of adenine is considered unlikely. However, it has been shown by Peeters et al. (2003) that in UV-shielded environments such as DCs, the half-life due to UV radiation is 8.3 Myr which would favor the accumulation of adenine. However, the fast proton component of the GCR is not attenuated in these environments, and when this is taken into account, the additional destruction of adenine from MeV protons reduces the overall lifetime by $\sim 30\%$ to ~ 6 Myr—approximately the lifetime of a star-forming molecular cloud. Therefore, approximately half of any initial population of adenine would then still be present over the lifetime of a typical dark cloud such as TMC-1. Further, it is noted that the destructive effects of both UV photons and high-energy charged particles are reduced by the outer layers of icy grains or icy bodies. In the latter case, it is expected that only the outer few meters would be effectively processed; the underlying material should be unprocessed over the age of our solar system, meaning that the abundance of adenine as well as other biomolecules would be unaltered from their composition within the pre-solar interstellar cloud from which our solar system formed. Hence, it is considered very likely that large icy bodies enabled the survival of biologically important species, which could occasionally be perturbed into the inner solar system to seed the primordial Earth.

Also, we have demonstrated that adenine is well shielded by a thin (~ 500 nm) layer of molecular oxygen and proposed two competing chemical pathways which lead to the formation of epoxides and carbonyls via adenine–oxygen interactions inside ices at 10 K. In true interstellar ice, trace amounts of adenine would likely be trapped in a polar ice matrix which is predominantly comprised of H_2O . However, it is predicted that in cold dense interstellar clouds, an outer apolar layer exists which is mostly thought to be O_2 , with substantial amounts of N_2 and CO also present (Ehrenfreund et al. 1992). As observed here, the decay rate of adenine is reduced by two orders of magnitude when shielded by a thin layer of O_2 —evidence that these apolar layers may help preserve biomolecular species that are contained within the polar regions of these ices. Orzechowska et al. (2007) have demonstrated that water ice can also serve to shield biomolecules formed within the polar ice regions from interstellar radiation. It is noted that typical interstellar ice constituents are known to be sources of molecular and atomic oxygen. Previous investigations within our group on the interaction of energetic electrons with low-temperature ices suggested that water (H_2O) can undergo fragmentation upon radiolysis to form excited state O atoms and H_2 via retro-insertion (Zheng et al. 2006). Likewise, a retro-insertion mechanism in CH_3OH exposed to energetic electrons leads to electronically excited oxygen atoms and CH_4 (Bennett et al. 2007). Finally, depending on the ice matrix conditions, CO can also be fragmented to a carbon and an oxygen atom (Bennett

et al. 2009). Suprathermal oxygen atoms produced by any of these mechanisms could then react with embedded adenine molecules, and the formation of epoxides and carbonyls as described above is therefore considered to be astrophysically relevant. As noted earlier, the interaction between oxygen atoms and adenine can also be used to predict what compounds may form if adenine were surrounded by a different matrix/molecules. To give one such example, in the case of epoxide formation, it is noted that the O atom is isoelectronic with both CH_2 or NH open-shell radical species, and the corresponding products would expect to form in the presence of a methane or ammonia matrix, respectively. It is therefore desirable for future work to incorporate the effects of different matrix compositions not only on the products that can be formed, but also on the decomposition rates of adenine to fully understand its survivability within these environments.

N.L.E. and S.U. acknowledge the Donors of the American Chemical Society Petroleum Research Fund (grant ACS-PRF no 44110-G6) and the National Science Foundation (award no CHE-0924456) for partial support of this research. N.L.E. thanks the Franklin College of Arts and Sciences and the Department of Physics and Astronomy at the University of Georgia for covering travel expenses. C.J.B. and R.I.K. thank the National Aeronautics Space Administration (NASA Astrobiology Institute under Cooperative Agreement No. NNA09DA77A issued through the Office of Space Science).

REFERENCES

- Allamandola, L. J., Tielens, A. G. G. M., & Barker, J. R. 1989, *ApJS*, **71**, 733
 Anders, E. 1989, *Nature*, **342**, 255
 Balucani, N., Asvany, O., Huang, L. C. L., Lee, Y. T., Kaiser, R. I., Osamura, Y., & Bettinger, H. F. 2000, *ApJ*, **545**, 892
 Bar-Nun, A., Bar-Nun, N., Bauer, S. H., & Sagan, C. 1970, *Science*, **168**, 470
 Bennett, C. J., Chen, S.-H., Sun, B.-J., Chang, A. H. H., & Kaiser, R. I. 2007, *ApJ*, **660**, 1588
 Bennett, C. J., Jameison, C. S., & Kaiser, R. I. 2009, *ApJS*, **182**, 1
 Bennett, C. J., Jameison, C. S., Mebel, A. M., & Kaiser, R. I. 2004, *Phys. Chem. Chem. Phys.*, **6**, 735
 Bennett, C. J., Jamieson, C. S., Osamura, Y., & Kaiser, R. I. 2006, *ApJ*, **653**, 792
 Bennett, C. J., & Kaiser, R. I. 2005, *ApJ*, **635**, 1362
 Bennett, C. J., Osamura, Y., Lebar, M. D., & Kaiser, R. I. 2005, *ApJ*, **634**, 698
 Bernstein, M. P., Dworkin, J. P., Sandford, S. A., Cooper, G. W., & Allamandola, L. J. 2002, *Nature*, **416**, 401
 Bernstein, M. P., Sandford, S. A., & Allamandola, L. J. 2005, *ApJS*, **161**, 53
 Blanco, F., & García, G. 2007, *Phys. Lett. A*, **360**, 707
 Boocock, G., & Cvetanović, R. J. 1961, *Can. J. Chem.*, **39**, 2436
 Borquez, E., Cleaves, H. J., Lazcano, A., & Miller, S. L. 2005, *Orig. Life Evol. Biosph.*, **35**, 79
 Botta, O., & Bada, J. 2002, *Surv. Geophys.*, **23**, 411
 Brack, A. 1999, *Adv. Space Res.*, **24**, 417
 Bredy, R., Bernard, J., Chen, L., Montagne, G., Li, B., & Martin, S. 2009, *J. Chem. Phys.*, **130**, 114305
 Brown, R. D., Godfrey, P. D., McNaughton, D., & Pierlot, A. P. 1989, *Chem. Phys. Lett.*, **156**, 61
 Brownlee, D., et al. 2004, *Science*, **304**, 1764
 Brownlee, D., et al. 2006, *Science*, **314**, 1711
 Cáceres, D., Bertin, M., Lafoose, A., Domaracka, A., Pliszka, D., & Azria, R. 2006, in AIP Conf. Proc. 876, The Physics of Ionized Gases: 23rd Summer School and International Symposium on the Physics of Ionized Gases, ed. L. Hadzievski, B. Marinkovic, & N. Simonovic (Melville, NY: AIP), 112
 Cecchi-Pestellini, C., Scappini, F., Saija, R., Iati, M. A., Giusto, A., Aiello, S., Borghese, F., & Denti, P. 2004, *Intl. J. Astrobiology*, **3**, 287
 Chakrabarti, S., & Chakrabarti, S. K. 2000, *A&A*, **354**, L6
 Charnley, S. B., Ehrenfreund, P., & Kuan, Y.-J. 2001, *Spectrochim. Acta A*, **57**, 685
 Charnley, S. B., et al. 2005, *Adv. Space Res.*, **36**, 137
 Chyba, C. F. 1990, *Nature*, **348**, 113
 Chyba, C. F., & Sagan, C. 1992, *Nature*, **355**, 125

- Chyba, C. F., Thomas, P. J., Brookshaw, L., & Sagan, C. 1990, *Science*, **249**, 366
- Cohen, M., & Kuhl, L. W. 1979, *ApJS*, **41**, 743
- Cosby, P. C. 1993, *J. Chem. Phys.*, **98**, 9560
- Darnell, J. E., & Doolittle, W. F. 1986, *Proc. Natl. Acad. Sci. USA*, **83**, 1271
- Drouin, D., Couture, A. R., Joly, D., Tastet, X., Aimez, V., & Gauvin, R. 2007, *Scanning*, **29**, 92
- Dworkin, J. P., Lazcano, A., & Miller, S. L. 2003, *J. Theor. Biol.*, **222**, 127
- Ehrenfreund, P., Breukers, R., d'Hendecourt, L., & Greenberg, J. M. 1992, *A&A*, **260**, 431
- Ehrenfreund, P., & Charnley, S. B. 2000, *ARA&A*, **38**, 427
- Elsila, J. E., Glavin, D. P., & Dworkin, J. P. 2009, *Meteoritics Planet. Sci.*, **44**, 1323
- Evans, N. L., & Ullrich, S. 2010, *J. Phys. Chem. A*, **114**, 11225
- Fegley, B., Prinn, R. G., Hartman, H., & Watkins, G. H. 1986, *Nature*, **319**, 305
- Freeland, S. J., Knight, R. D., & Landweber, L. F. 1999, *Science*, **286**, 690
- Ghosh, K. K., & Ghosh, S. N. 1980, *Life Sci. Space Res.*, **18**, 37
- Gibb, E. L., Whittet, D. C. B., Boogert, A. C. A., & Tielens, A. G. G. M. 2004, *ApJS*, **151**, 35
- Gilbert, W. 1986, *Nature*, **319**, 618
- Glaser, R., Hodgen, B., Farrelly, D., & McKee, E. 2007, *Astrobiology*, **7**, 455
- Glavin, D. P., Schubert, M., & Bada, J. L. 2002, *Anal. Chem.*, **74**, 6408
- Greenberg, J. M. 1989, *Adv. Space Res.*, **9**, 15
- Griffith, R. W. 2009, *Orig. Life Evol. Biosph.*, **39**, 517
- Gu, J., Tian, A., Li, W. K., & Wong, N. B. 2000, *J. Phys. Chem. B*, **104**, 10692
- Gu, X., Zhang, F., & Kaiser, R. I. 2008, *J. Phys. Chem. A*, **112**, 9607
- Hawkins, M., & Andrews, L. 1983, *J. Am. Chem. Soc.*, **105**, 2523
- Hill, A., & Orgel, L. E. 2002, *Orig. Life Evol. Biosph.*, **32**, 99
- Holtom, P. D., Bennett, C. J., Osamura, Y., Mason, N. J., & Kaiser, R. I. 2005, *ApJ*, **626**, 940
- Ikehara, K. 1999, *Seibutsu Kagaku*, **51**, 43
- Isaacson, M. 1972, *J. Chem. Phys.*, **56**, 1813
- Jamieson, C. S., Mebel, A. M., & Kaiser, R. I. 2006, *ApJS*, **163**, 184
- Jochims, H. W., Schwelb, M., Baumgärtel, H., & Leach, S. 2005, *Chem. Phys.*, **314**, 263
- Kaiser, R. I., Eich, G., Gabrysch, A., & Roessler, K. 1997, *ApJ*, **484**, 487
- Kaiser, R. I., Ochsenfeld, C., Stranges, D., Head-Gordon, M., & Lee, Y. T. 1998, *Faraday Discuss*, **109**, 183
- Kaiser, R. I., & Roessler, K. 1998, *ApJ*, **503**, 959
- Kilday, M. V. 1978, *J. Res. National Bureau of Standards*, **83**, 347
- Kim, Y. S., Bennett, C. J., Chen, L.-H., O'Brien, K., & Kaiser, R. I. 2010, *ApJ*, **711**, 744
- Kobayashi, K., Kasamatsu, T., Kaneko, T., Koike, J., Oshima, T., Saito, T., & Yanagawa, H. 1995, *Adv. Space Res.*, **16**, 21
- Lacey, J. C., Cook, G. W., & Mullins, D. W. 1999, *Chemtracts*, **12**, 398
- Lafosse, A., Bertin, M., Domaracka, A., Pliszka, D., Illenberger, E., & Azria, R. 2006, *Phys. Chem. Chem. Phys.*, **8**, 5564
- Levy, M., & Miller, S. L. 1998, *Proc. Natl. Acad. Sci. USA*, **95**, 7933
- Levy, M., & Miller, S. L. 1999, *J. Mol. Evol.*, **48**, 631
- Lin, J., Yu, C., Peng, S., Akiyama, I., Li, K., Kao Lee, L., & LeBreton, P. R. 1980, *J. Am. Chem. Soc.*, **102**, 4627
- Liu, J., Xu, T., & Fu, Y. 2005, *J. Non-Cryst. Solids*, **351**, 3050
- Loeffler, M. J., Raut, U., Vidal, R. A., Baragiola, R. A., & Carlson, R. W. 2006, *Icarus*, **180**, 265
- Magee, J. L., & Chatterjee, A. 1987, *Radiation Chemistry: Principles and Applications*, ed. Farhatziz & M. A. J. Rodgers (New York: VCH)
- Martin, S., Bredy, R., Allouche, A. R., Bernard, J., Salmoun, A., Li, B., & Chen, L. 2008, *Phys. Rev. A*, **77**, 062513
- Martins, Z., et al. 2008, *Earth Planet. Sci. Lett.*, **270**, 130
- Mattioda, A. L., Hudgins, D. M., Bauschlicher, C. W., Rosi, M., & Allamandola, L. J. 2003, *J. Phys. Chem. A*, **107**, 1486
- Miller, S. L. 1953, *Science*, **117**, 528
- Milligan, D. E., & Jacox, M. E. 1967, *J. Chem. Phys.*, **47**, 278
- Muñoz Caro, G. M., et al. 2002, *Nature*, **416**, 403
- Nowak, M. J., Lapinski, L., Kwiatkowski, J. S., & Leszczynski, J. 1996, *J. Phys. Chem.*, **100**, 3527
- Nuevo, M., Auger, G., Blanot, D., & d'Hendecourt, L. 2008, *Orig. Life Evol. Biosph.*, **38**, 37
- Nuevo, M., Chen, Y.-J., Yih, T.-S., Ip, W.-H., Fung, H.-S., Cheng, C.-Y., Tsai, H.-R., & Wu, C.-Y. R. 2007, *Adv. Space Res.*, **40**, 1628
- Nuevo, M., Milam, S. N., Sandford, S. A., Elsila, J. E., & Dworkin, J. P. 2009, *Astrobiology*, **9**, 683
- Orgel, L. E. 2004, *Crit. Rev. Biochem. Mol. Biol.*, **39**, 99
- Oró, J. 1960, *J. Biochim. Biophys. Res. Commun.*, **2**, 407
- Oró, J., & Kimball, A. P. 1962, *Arch. Biochem. Biophys.*, **96**, 293
- Orzechowska, G. E., Goguen, J. D., Johnson, P. V., Tsapin, A., & Kanik, I. 2007, *Icarus*, **187**, 584
- Palumbo, M. E., Baratta, G. A., Fulvio, D., Garozzo, M., Gomis, O., Leto, G., Spinella, F., & Strazzulla, G. 2008, *J. Physics: Conf. Ser.*, **101**, 1
- Panajotović, R., Michaud, M., & Sanche, L. 2007, *Phys. Chem. Chem. Phys.*, **9**, 138
- Parker, J. K., & Davis, S. R. 1999, *J. Am. Chem. Soc.*, **121**, 4271
- Peeters, Z., Botta, O., Charnley, S. B., Kisiel, Z., Kuan, Y.-J., & Ehrenfreund, P. 2005, *A&A*, **433**, 583
- Peeters, Z., Botta, O., Charnley, S. B., Ruitkamp, R., & Ehrenfreund, P. 2003, *ApJ*, **593**, L129
- Pilling, S., Seperuelo Duarte, E., da Silveira, E. F., Balanzat, E., Rothard, H., Domaracka, A., & Boduch, 2010, in *Astrobiology Science Conf. 2010: Evolution and Life: Surviving Catastrophes and Extremes on Earth & Beyond* (LPI Contribution No. 1538), **5181**
- Ponnamperuma, C., Lemmon, R. M., Mariner, R., & Calvin, M. 1963, *Proc. Natl. Acad. Sci. USA*, **49**, 737
- Poole, A. M., Jeffares, D. C., & Penny, D. 1998, *J. Mol. Evol.*, **46**, 1
- Prasad, S., & Tarafdar, S. P. 1983, *ApJ*, **267**, 603
- Ricci, A., Bauschlicher, C. W., & Bakes, E. L. O. 2001, *Icarus*, **154**, 516
- Rice, J. M., & Dudek, G. O. 1967, *J. Am. Chem. Soc.*, **89**, 2719
- Rimola, A., & Ugliengo, P. 2009, *Phys. Chem. Chem. Phys.*, **11**, 2497
- Rode, B. M. 1999, *Peptides*, **20**, 773
- Roy, D., Najafian, K., & Schleyer, P. v-R. 2007, *Proc. Natl. Acad. Sci. USA*, **104**, 17272
- Saladino, R., Crestini, C., Costanzo, G., Negri, R., & Di Mauro, E. 2001, *Bioorganic Medicinal Chem.*, **9**, 1249
- Satoshi, K., Takayanagi, M., & Nakata, M. 1997, *J. Mol. Struct.*, **413**, 365
- Satzger, H., Townsend, D., Zgierski, M. Z., Patchkovskii, S., Ullrich, S., & Stolow, A. 2006, *Proc. Natl. Acad. Sci. USA*, **103**, 10196
- Sekanina, Z., & Yeomans, D. K. 1985, *AJ*, **85**, 2335
- Shapiro, R. 1995, *Orig. Life Evol. Biosph.*, **25**, 83
- Simakov, M. B., & Kuzicheva, E. A. 2005, *Adv. Space Res.*, **36**, 190
- Smith, I. W. M., Talbi, D., & Herbst, E. 2001, *A&A*, **369**, 611
- Socrates, G. 2001, *Infrared and Raman Characteristic Group Frequencies* (3rd ed.; New York: John Wiley & Sons, Inc.)
- Steinfeld, J. I., Francisco, J. S., & Hase, W. L. 1999, *Chemical Kinetics and Dynamics* (2nd ed.; Englewood Cliffs, NJ: Prentice Hall)
- Taatjes, C. A., et al. 2010, *J. Phys. Chem. A*, **114**, 3355
- Tait, J. F. K., Edwards, H. G. M., Farwell, D. W., & Yarwood, J. 1995, *Spectrochim. Acta A*, **51**, 2101
- Teolis, B. D., Loeffler, M. J., Raut, U., Famá, M., & Baragiola, R. A. 2007, *Icarus*, **190**, 274
- Teolis, B. D., Shi, J., & Baragiola, R. A. 2009, *J. Chem. Phys.*, **130**, 134704
- Tielens, A. G. G. M. 2008, *ARA&A*, **46**, 289
- Zhang, F., Kim, S., Kaiser, R. I., Jamal, A., & Mebel, A. 2009, *J. Chem. Phys.*, **130**, 234308
- Zheng, W., Jewitt, D., & Kaiser, R. I. 2006, *ApJ*, **639**, 534
- Ziegler, J. F., Biersack, J. P., & Littmark, V. 1985, *The Stopping and Range of Ions in Solids* (New York: Pergamon)